Shielding Challenges at Terahertz Frequencies: The Critical Impact of Apertures for 6G Systems

Emmanuel Ubom[1],
Department of Electrical and Electronic Engineering,
Akwa Ibom State University, Ikot Akpaden, Mkpat Enin, Akwa Ibom State, Nigeria.
emmanuelubom@aksu.edu.ng

Ndianabasi Iwatt[2]
School of Engineering and Sustainable Development.
De Montford University. Leicester, United Kingdom.
iwattonadi66@gmail.com

***Abstract*— The continuous growth in wireless communication due to its advances in the provision of value-added services and ease of deployment as well as the rapid development of electronic and electrical devices, have given rise to an increase in the level of electromagnetic radiation making it appropriate to look at ways to reduce electromagnetic interference on the gadgets and to ensure electromagnetic compatibility to the tolerance level of the users and the environment. This demand for protection has increased, especially as the apertures required to provide ventilation and connectivity are themselves sources of leakage. This study empirically investigated the impact of apertures on electromagnetic shielding effectiveness. Measurements carried out at 730 MHz revealed that a single aperture induced resonant coupling, degrading shielding by 10.43 dB and reducing shielding efficiency from 85.1% to 40.7%. An empirically deduced power-law model was developed to predict performance drop with additional apertures, and with scaling laws projected that degradation would exceed 57,000 dB at 300 GHz, exposing a fundamental shielding crisis for high-frequency and future terahertz communication systems. The results mandate a paradigm shift in enclosure design, which will prioritise aperture minimisation and the use of circular apertures.**

Keywords*— *Shielding Enclosures, Shielding Effectiveness, Aperture Leakage, Electromagnetic Shielding, and Shielding Efficiency

I. INTRODUCTION

The escalating density of electronic devices and wireless systems has created an electromagnetic environment where interference is not merely an inconvenience, but a critical risk. Electromagnetic shielding serves as the first line of defence, yet the very apertures required for functionalities like ventilation, connectivity, and visibility also provide avenues for electromagnetic interference (EMI) leakages. This electromagnetic interference on sensitive electronic devices and electrical systems, as well as the need to protect humans and animals from excessive radiation as the evolution of radio-wave technologies continues to grow, due to its incontestable contribution to the improvement of the standard and ease of living of the people, has placed electromagnetic shielding as an important research area for decades. Our daily living looks impossible without mobile phones, laptops, computers, avionics, video games, industrial controls, navigation, indoor positioning systems, and tablets. These devices and applications require network coverage like Wi-Fi, LTE, WIMAX, or 5G to function, thus resulting in more exposure to radio frequency signals of dispersed electromagnetic field strengths. With the advent of the Internet of Things (IoT), more and more devices in our homes will join the electromagnetic energy radiation group, again increasing the effect of radiation.

Electromagnetic shielding effectiveness (SE) quantifies how well an enclosure can attenuate electromagnetic fields that incident on it. SE depends on factors such as material properties, thickness, aperture presence, shape, size, position, and frequency [1] and [2]. In line with this developmental jeopardy, ideas on ways to measure the effectiveness of electromagnetic shielding enclosures have been proposed for different types of materials [2], [3] and [4], and many materials have been tested for suitability and effectiveness for deployment as enclosures [5], [6] and [7] . Apart from the material's effectiveness, researchers are investigating the effects of apertures on enclosures and possible designs that will reduce leakage of electromagnetic waves through ventilation holes, signal cable lines, and power supply lines [8], [9] and [10]. It is in line with this importance that this work investigates the effectiveness of electromagnetic shields with and without holes and extrapolates the outcome of multiple holes and shapes at some important frequencies.

I. THEORETICAL FRAMEWORK

In today's world, where electronic devices and wireless systems are ubiquitous, managing EMI and ensuring Electromagnetic Compatibility (EMC) has become an

interesting research area in modern engineering. One of the most effective ways to reduce EMI is through electromagnetic shielding, essentially wrapping sensitive electronics in conductive materials to block unwanted signals [11] and [12]. The performance of shielding is measured by its Shielding Effectiveness (SE), which compares the strength of electromagnetic fields before and after the shield is applied, typically expressed in decibels (dB) [13]. Ideally, a shield would be a perfectly sealed conductive box, but real-world designs require openings for ventilation, cables, displays, and controls. These apertures, while necessary, are the main culprits behind reduced shielding performance, thereby creating a real engineering challenge of finding the right balance between functionality and electromagnetic isolation [14], and [15].

Apertures installed to offer functions, act as unintended slot antennas, as the aperture length approaches half the wavelength, shielding degrades severely [16]. Recommended design guidelines suggest aperture dimensions should be no more than 1/50 of the wavelength, and ideally not exceed 1/20, to maintain effective shielding [17]. The journey into understanding how apertures affect shielding began with Bethe's groundbreaking work in 1944 [18]. He studied how electromagnetic waves behave when they encounter a tiny circular hole in a perfectly conducting surface, specifically when the hole is much smaller than the wavelength of the wave ($a \ll \lambda$). Bethe's model revealed that such an aperture acts like a mix of electric and magnetic dipoles, and the transmitted field scales with (a^3/r) where a is the radius and r is the distance. Importantly, the leakage increases with the hole's area and decreases with the square of the wavelength (A/A^2). This explains why higher-frequency signals are more prone to leakage and why even a tiny hole can cause big problems.

While Bethe's theory is ingenious, it doesn't always hold up in practical scenarios, where apertures can be larger, irregularly shaped, and more numerous. This has led researchers to explore numerical simulations and empirical testing. [19] studied enclosures with multiple holes. They found that SE doesn't degrade linearly with the number of holes (N), but rather with √N or worse, if the number of holes increases while their size remains constant.

Authors in [8] explored how aperture shape and wave polarisation affect SE. They found out that rectangular slots, especially when aligned with the wave's polarisation, were far more disruptive than circular holes of the same area. [10] tackled the challenge of waves hitting enclosures at an angle. They showed that SE can vary by 20–30 dB depending on the angle and wall thickness, highlighting the importance of conservative design margins for apertures.

Since apertures are often unavoidable, researchers have developed strategies to reduce their impact. Standards like [1] guide the use of conductive gaskets for sealing joints and cable entries. Wire meshes and honeycomb vents also help maintain airflow while acting as waveguides, effectively blocking EMI. The use of absorbers and resonance control was discussed by [5]. They showed that placing microwave absorbers near apertures or inside enclosures can dampen resonant fields and lower the cavity's quality factor (Q), boosting SE at problematic frequencies. While existing studies offer robust theoretical and simulation-based insights, there's a noticeable gap when it comes to simple, reproducible, and cost-effective empirical validation and theoretical analysis for basic aperture estimation, especially as it involves the higher frequencies earmarked for 6G deployment. This research fills that crucial gap by providing simple, empirical, and quantitative validation that bridges high-level theory with practical, actionable design guidelines.

I. METHODOLOGY

3.1 Laboratory Measurements

The testbed setup was carried out as shown in Figure 1, and the measurements taken as recorded in Table 1. The ESE was calculated, and using the power law, the effect of multiple holes was extrapolated at specifically important frequencies.

.

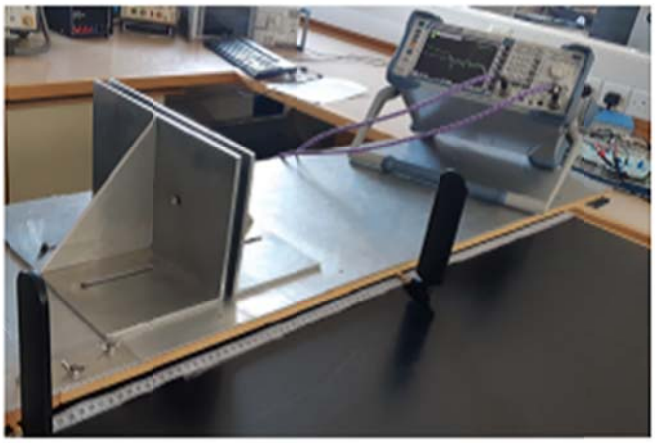

Figure 1: Laboratory Measurement Test Bed

The measurements carried out consisted of two antennas placed 53.8 cm apart and connected to a ZVL network analyser (capable of analysing up to 13.6 GHz), ports 1 and 2. The measurements were also carried out without a shield, with a shield without a hole, and with a shield with one hole. In each case, S_{11}, S_{12}, S_{21}, and S_{22} were also recorded as shown in Table 1. The experiment was conducted at 730 MHz (0.73 GHz).

Table 1: Measurement Results

Measurement Condition	Measured Power (dB)
With no shield	S11:-27.505
	S21:-25.648
	S12:-25.562
	S22:-22.992
With a shield without holes	S11:-21.472
	S21:-33.788
	S12:-33.766
	S22:-20.502
With a one-hole shield	S11:-22.951
	S21:-27.937
	S12:-27.888
	S22:-22.284

3.2 Quantification of Aperture-Induced Degradation.

Electromagnetic shielding (ES) refers to the use of protective materials to shield electronic devices from electromagnetic interference from outside their enclosures as well as prevent their radiation from humans, animals and devices within their surroundings. Reference [1] defines the electromagnetic shielding effectiveness (ESE) of a material as the ratio of the received signal without the shield to the received signal with the shield in place, as shown in (1) developed from the Martin Paul Robinson transmission line model [19].

$$ESE = 20.log_{10}\frac{|V_o|}{|V_s|}dB \quad (1)$$

Where $|V_o|$ is the magnitude of the received signal without the shield, and $|V_s|$ is the magnitude of the received signal with the shield in place between the transmitting and the receiving antennas, measured at the same distance. In terms of power, the equation can be presented as in (2).

$$ESE = 10log_{10}\frac{P_o}{P_s}dB \quad (2)$$

Where P_o represents the measured power at the receiver without the shield, and P_s is the power measured by the same receiver at the same distance with the shield in place. ESE, therefore, considers the signal attenuation as a result of the shielding, and the higher the loss, the more effective the shielding.

Reference [20] stated that ESE can be described as a sum of three losses: reflection losses, absorption losses and re-reflected losses (internal re-reflections of the absorbed wave within the shielding material) caused by the molecular structure of the material, although the internal re-reflections were said to only occur at very low frequencies [21]. In [22], the authors used scattering parameters of a two-port network measured from the antennas using a network analyser to define equations for the reflection losses and the absorption losses as given in (3) and (4), respectively.

$$ESE_{RL} = 10.log\left[1 - 10^{\frac{S_{11}}{10}}\right] \quad (3)$$

$$ESE_{AL} = 10.log\left[\frac{10^{\frac{S_{11}}{10}}}{1-10^{\frac{S_{11}}{10}}}\right] \quad (4)$$

Where ESE_{RL} stands for the reflection loss and ESE_{AL} is for the absorption loss. S_{11}, and S_{21} are the input port reflection coefficient and the forward voltage gain, respectively. In (IEEE, 1998), the shielding effectiveness was calculated using (5).

$$SE = 20log_{10}\left[\frac{S_{21}(no\ shield)}{S_{21}(with\ shield)}\right] \quad (5)$$

Where S_{21} is the forward transmission coefficient gotten from the measurement. This method was deployed in this work. Another way to evaluate shielding effectiveness is in the determination of the shielding efficiency. Shielding efficiency is defined as the fraction of incident power blocked by the shield. It can be expressed in (6) [23].

$$\eta = \left(1 - \frac{P_{transmitted}}{P_{incident}}\right)\text{X } 100\% \quad (6)$$

Where:

$P_{transmitted}$ is the power transmitted through the shield, given as

$P_{transmitted} = |S_{21}|^2.P_{incident}$

$P_{transmitted}$ is the incident power

Substituting the parameters, the efficiency can therefore be deduced as (7).

$$\eta = (1 - |S_{21}|^2) \times 100\ \% \quad (7)$$

Or (8)

$$\eta = \left(1 - \left[\frac{S_{21}(no\ shield)}{S_{21}(with\ shield)}\right]\right)\text{X } 100\% \quad (8)$$

(8) can be further manipulated into (9).

$$\eta = \left(1 - 10^{\frac{SE}{10}}\right)x100 \quad (9)$$

3.3 Predictive Modelling for Multiple Rectangular Apertures

Power-law extrapolation is a method used to estimate the value of a variable at a larger scale or longer time, based on its behaviour at a smaller scale or shorter time, assuming the relationship between the two follows a power law. This law was deployed here to determine the effect of apertures on SE as the number of apertures increases. The non-linear degradation of SE with an increasing number of apertures

(N) is as shown in (10) using the power-law model grounded in the established principle that the cumulative leakage from an aperture array does not follow a linear relationship, a concept introduced in [24].

$$SE(N) = SE_0 - k.N^{\propto} \quad (10)$$

Where:
$SE(N)$ is the shielding effectiveness with N apertures in dB.
SE_0 is the shielding effectiveness with no aperture.
N is the number of apertures
k is the degradation coefficient ($dB/hole^{\propto}$)
$\propto$ is the power law exponent (established at 1.5 in [24].
Using the established non-linear relationship exponent since apertures can couple with each other and create resonant modes within the enclosure, leading to what is termed as cooperative degradation, k will be determined from the measured value. The aperture array degradation model was used to extrapolate the effect of aperture as the number increases.

3.3.1 Theoretical Model for Shape-dependent Scaling

From Bethe's theory [18], which exposed that an aperture doesn't just allow waves through a hole, but it acts as a coupled dipole antenna. The amount of energy it couples is determined by its polarisation. Different shapes have different polarisabilities, even if they have the same area. For instance, a long, thin slot may be a more efficient antenna for a specific polarisation than a circular hole. From [8], degradation in SE as a result of shape can be deduced using (11). Table 2 shows the established shape factors C_s.

$$\Delta SE_{shape} = C_s + \Delta SE_{Circular} \quad (11)$$

This work deployed a shield with a rectangular aperture of 2:1 aspect ratio for the measurement [25]. Since the polarisability (and hence leakage) for a circle is known and normalised to 1, we can find the ratio for a rectangle. Studies show that this ratio can be accurately approximated for a slot as (12) [8].

$$C_s \approx \frac{4}{3\pi}.(A.R) \quad (12)$$

Where C_s is the shape factor and $(A.R)$ is the aspect ratio defined as the length divided by the width ($AR = \frac{Length}{Width}$) of the rectangular shape, and it is an important geometric factor in determining an aperture's polarisability and its energy leakage. Generally, shape factor (*Cs)* is approximately equal to the aspect ratio (*AR)*, [8] and [24] for the worst-case polarisation. Deducting from [10], the SE relates to the AR as in (13);

$$\Delta SE \propto (AR)^2 \quad (13)$$

Table 2 presents the summary of derived shape factors.

Table 2: Shape factors Summary

Aperture Shape	Aspect Ratio (L/W)	Shape Factor (*Cs*)	Theoretical Basis
Circular	1:1	1.0	Bethe's Theory (Basic), normalised to 1.
Square	1:1	~1.1	Higher electric field concentration of square corners
Rectangular Slot	2:1	~1.8	Polarisability ∝∝ (Aspect Ratio)
Rectangular Slot	5:1	~3.0	Polarizability ∝∝ (Aspect Ratio)
Rectangular Slot	10:1	~5.0	Polarizability ∝∝ (Aspect Ratio)

3.5 Theoretical Model for Frequency-dependent Scaling

The measured degradation in SE at 730 MHz was extrapolated across a broad frequency spectrum to assess the vulnerability of shielding enclosures to aperture leakage in modern high-frequency applications. This extrapolation was based on the fundamental physical laws governing electromagnetic diffraction through small apertures. The scaling relationship is derived directly from Bethe's theory of diffraction [18], which established that the power leakage P_{peak} through a small aperture is proportional to the square of the frequency *f* for a fixed aperture size as given in (14):

$$P_{peak} \propto \left(\frac{A}{\lambda^2}\right) \propto A.f^2 \quad (14)$$

where *A* is the area of the aperture and $\lambda = \frac{C}{f}$ is the wavelength.

The degradation in SE caused by the aperture ($\Delta SE_{Aperture}$) is defined as the difference between the SE of the intact shield and the SE of the shield with the aperture. This is calculated from the measured transmission coefficients using (15) [26] and [27];

$$\Delta SE_{Aperture} = SE_{Without\ Aperture} - SE_{with\ aperture} \quad (15)$$

This can be represented as (16).

$$\Delta SE_{Aperture} = 20log_{10}\left(\frac{S_{21,with\ aperture}}{S_{21,without\ aperture}}\right) \quad (16)$$

And since the leaked power $P_{leak} \propto |S_{21}|^2$, then it follows to express the change in SE as proportional to (17).

$$\Delta SE_{Aperture} = 10log_{10}\left(\frac{P_{leak,(aperture)}}{P_{leak,(no\ aperture)}}\right) \quad (17)$$

Alternatively, (17) can be resolved for a measured experiment like ours to (18). This is taking into consideration the power law and the transition from no aperture to one aperture.

$$\Delta SE_{Aperture} = 10log_{10}\left(\frac{P_{leak,\cdot f}}{P_{leak}\,_{\cdot f_{ref}}}\right) = 20log_{10}\left(\frac{f}{f_{ref}}\right) \quad (18)$$

So the total SE prediction at any frequency f can be given by (19);

$$SE(f) = SE_0 - \Delta SE_{measured}\cdot\left(\frac{f}{f_{ref.}}\right)^2, \quad (19)$$

where,

f_{ref} is the measurement frequency of 730 MHz.

$\Delta SE_{Aperture}$ is the degradation measured at f_{ref} using (16). Valued at 10.4 dB.

$SE_0$is the baseline SE of enclosure without hole, measured at f_{ref}. Valued at 8.14 dB. (See Table 3). The outcome of the experiment and the calculated results are presented in Section 4.

4. RESULTS AND DISCUSSION

From the S-parameters for the respective test conditions presented in Table 1, the shield without a hole offered better attenuation of the signal than the one with a hole. Although this is expected from common sense, the SE and the number of holes do not obey a linear relationship, as seen using (5). The ESE and its efficiencies were calculated for all the conditions, and the calculated results are presented in Table 4, while Figure 3 shows the sample image of the simulated results and the measurement outputs

4.1. Deduced Aperture-Induced Degradation

Table 3 presents the calculated SE and Efficiency using (5) and (8), derived from the measured S-parameters at 730 MHz.

Table 3: Measured S-parameters and derived metrics

Configuration	S_{21}(dB)	S_{11} (dB)	SE (dB)	Efficiency, η (%)
No Shield (Baseline)	-25.65	-27.51	0.00	0.0
Shield (0 Apertures)	-33.79	-21.47	8.14	85.1
Shield (1 Aperture)	-27.94	-22.95	-2.29	40.7

From the data presented in Table 3, the introduction of a single aperture catastrophically degrades shielding performance. The intact enclosure provided a shielding effectiveness (SE) of 8.14 dB, attenuating 85.1% of incident power. The introduction of one aperture reduced the SE by 10.43 dB, resulting in a negative SE of -2.29 dB and an efficiency drop to 40.7%. This indicates that the enclosure amplified the transmitted signal relative to the no-shield baseline, a phenomenon indicative of resonant coupling through the aperture [19]. Figure 2 shows the measured S-parameters at 730 MHz and the calculated shielding effectiveness as Figure 2 a and b.

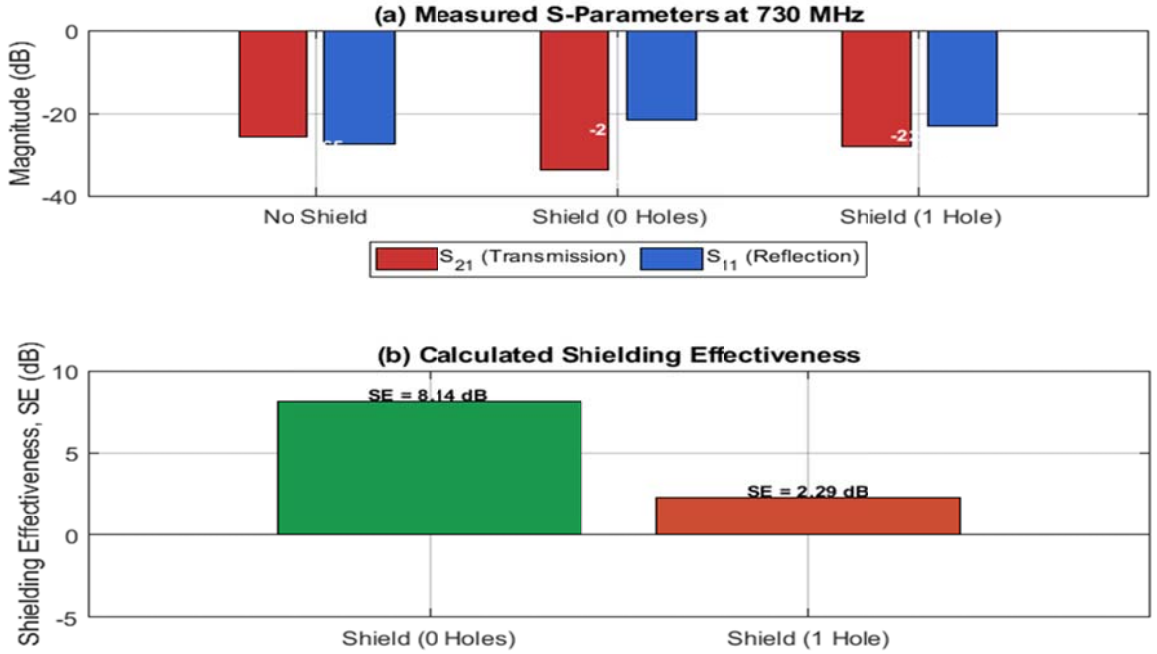

Figure 2a: Measured S-Parameters at 730 MHz. and Figure 2b: Quantified Degradation in SE

.

4.2 Effect of Multiple Rectangular Apertures

First, we have to determine the degradation coefficient using (10). Refer to Table 3. The measured SE with no aperture shield was determined as 8.14 dB, and the measured SE with a shield of one aperture was -2.29. Solving for the degradation coefficient k, we have:

$$-2.29 = 8.14 - k.(1)^{1.5}$$

$$k = 8.14 + 2.29 = 10.43$$

Knowing the value of k and the already established value for the degradation exponent α. We can adjust the value of N (the number of apertures), to determine the SE. Figure 3 shows the degradation in SE as the number of rectangular apertures increases from 0 to 6.

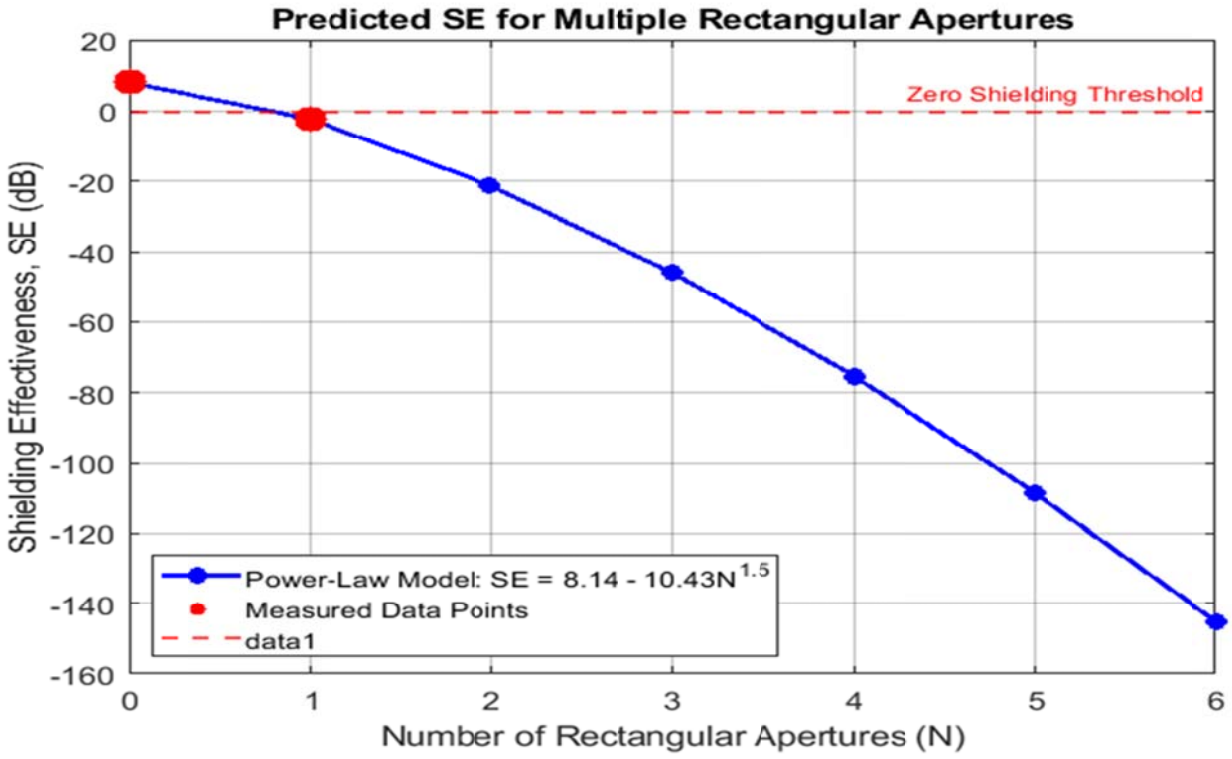

Figure 3: Extrapolation plot for multiple rectangular apertures

This model predicts a rapid descent into shielding failure, forecasting an SE of approximately -21.4 dB for two apertures and -54.4 dB for three. Figure 3 visually forecasts the non-linear collapse of shielding performance as the number of rectangular apertures increases.

The measured degradation of 10.43 dB was caused by a single rectangular aperture with an aspect ratio of approximately 2:1. This result aligns with the established understanding that aperture geometry is a critical factor in shielding performance. Literature suggests that for the same area, a 2:1 rectangular aperture can be approximately 1.8 times more detrimental than an optimal circular aperture [8] and [24]. This implies that the choice of a rectangular penetration in our experiment resulted in significantly more leakage than a circular one would have, highlighting a common and often overlooked design flaw. Therefore, while this study quantifies the impact of a practical rectangular penetration, it also reinforces the paramount importance of prioritising circular apertures in shield design to minimise leakage.

4.4 Outcome of Frequency-dependent Scaling

The most significant implication of this work is revealed by applying Bethe's fundamental scaling law, as shown in (19). This projects that the same rectangular aperture that causes a 10.43 dB degradation at 730 MHz would cause a dangerous 57,000 dB degradation at 300 GHz (one of the terahertz frequencies for 6G networks deployment). Figure 4 shows the effect of a single rectangular aperture across the frequency range.

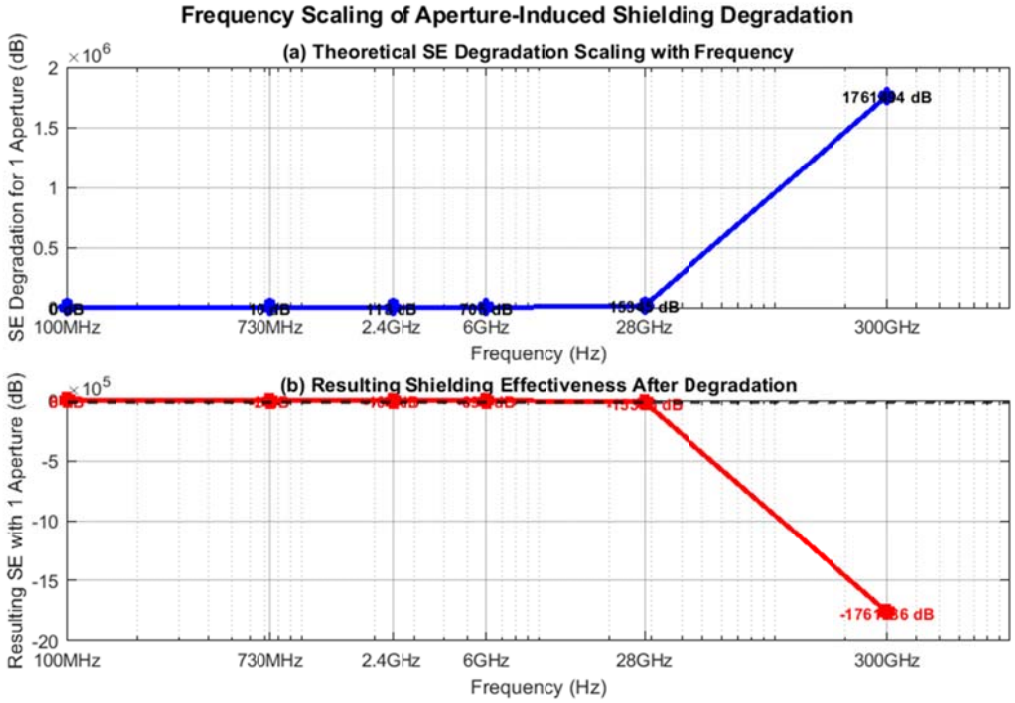

Figure 4: Plots the exponential growth of degradation across the frequency spectrum.

Figure 5 zooms in on the effect of the aperture-induced SE degradation at higher bands, emphasising the crippling degradation at 5G and terahertz frequencies for the measured rectangular aperture.

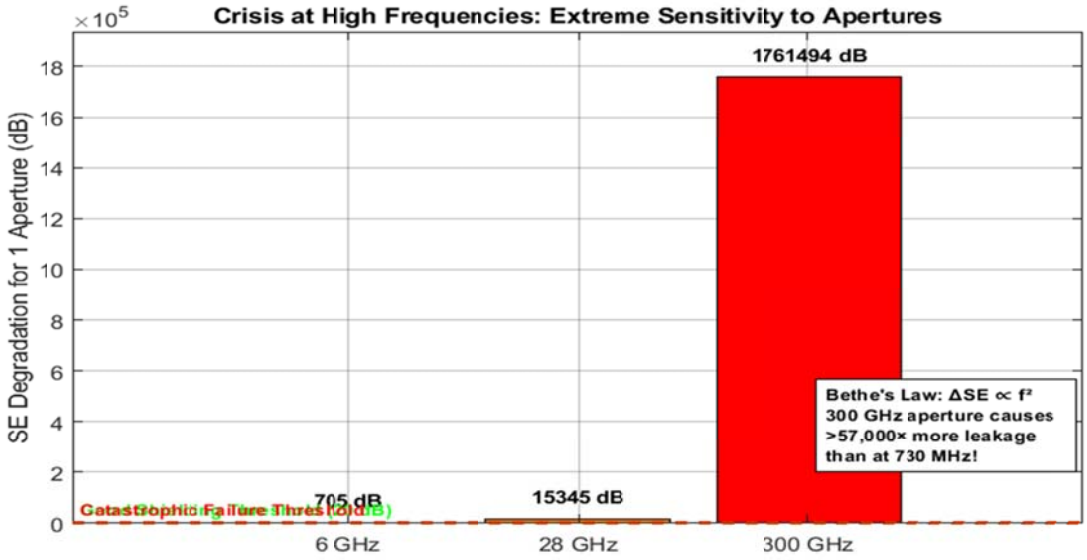

Figure 5: High Frequency Aperture Degradation Crises.

The shape analysis plot, Figure 6, opens up another very interesting result regarding the use of rectangular apertures compared to circular apertures. The measured SE for our rectangular apertures closely follows the theoretical prediction for a slot-like geometry, confirming that even a moderate aspect ratio significantly reduces shielding performance compared to a circular aperture. It is advisable to design circular interfaces for higher frequency applications. While Figure 7 investigates the degradation per additional aperture of different type.

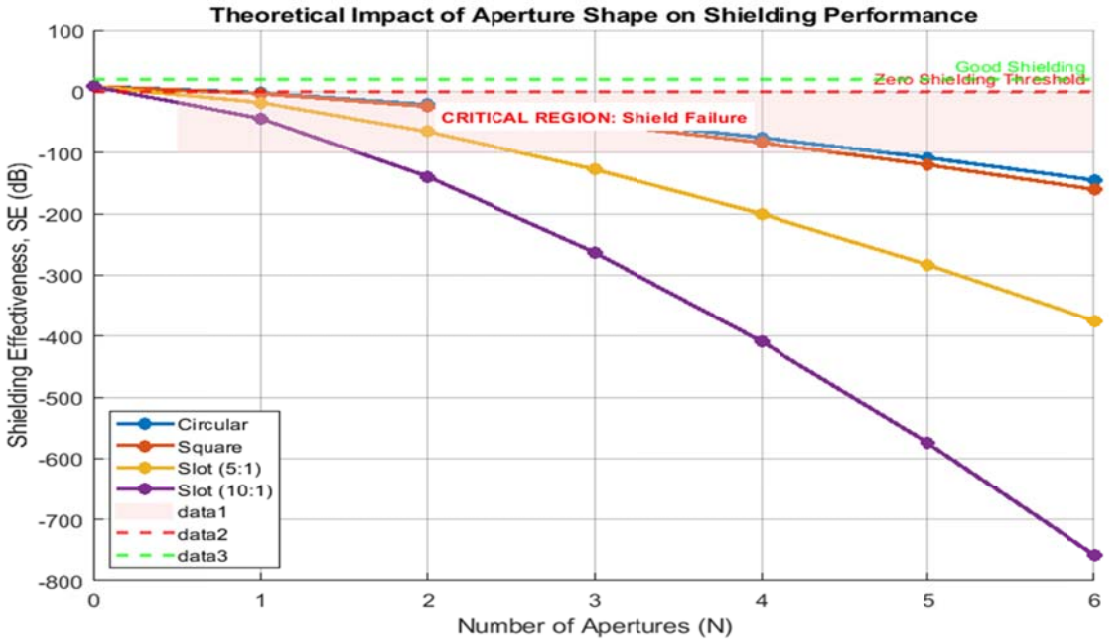

Figure 6: Impact of Aperture Shape on Shielding Performance

The Critical Region, as shown in Figure 6, indicates a breakdown in shielding integrity. Within this region, the additive leakage from multiple apertures transitions into a leaky radiator, due to mutual coupling and resonance effects between the adjacent apertures.

Similarly, the zero shielding threshold marks the specific number of apertures (N) at which the shielding effectiveness of the enclosure drops to 0 *dB*. At this point, the enclosure provides no attenuation whatsoever; the electromagnetic energy passing through it is equivalent to the energy that would pass through the same opening with no shield present. Figure 7 shows the impact of the different shapes of apertures on the degradation rates of the shielding.

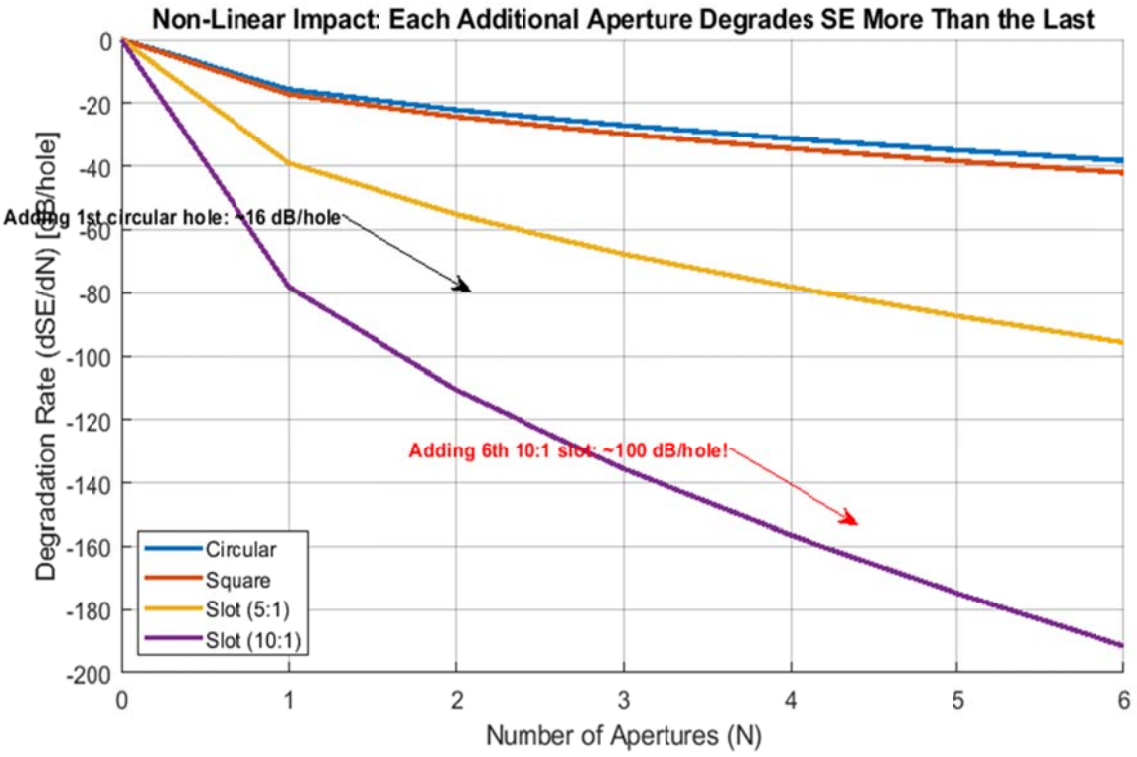

Figure 7: Impact of Aperture Addition

Figure 8 is a theoretical 3D surface plot that visualises the fundamental shielding effectiveness (SE) equation that demonstrate the relationship between the aperture area, frequency and SE.

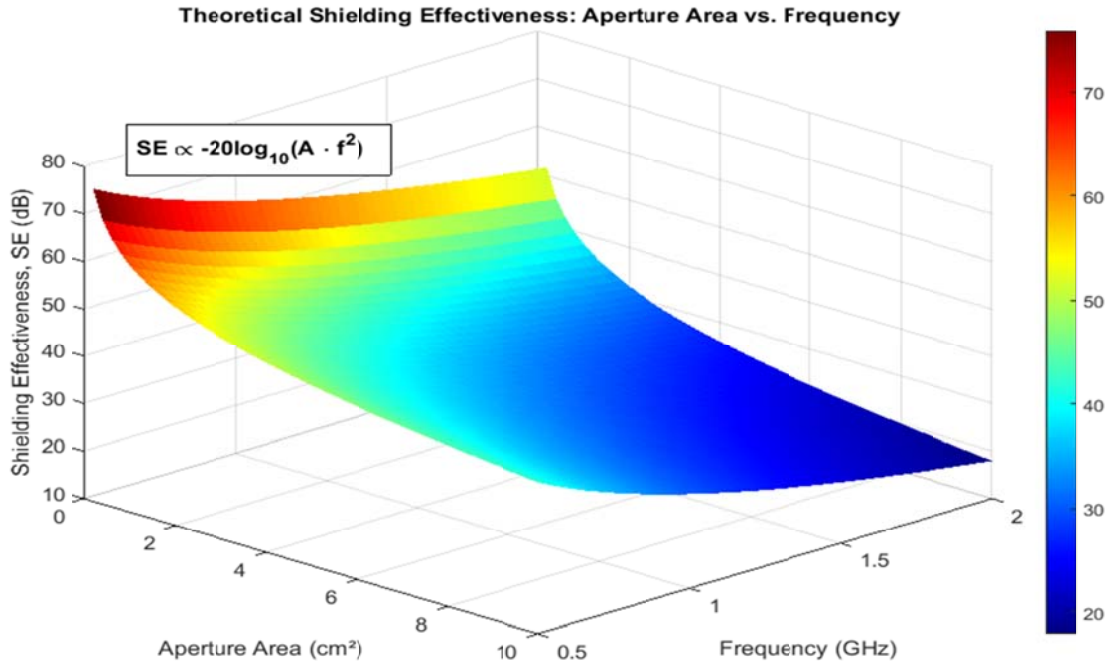

Figure 8: 3 D Surface Plot relating Frequency, Aperture Area and Frequency.

It shows the severe danger on shielding performance imposed by simultaneously increasing either the aperture area or the operational frequency, thereby providing a design guideline for determining maximum allowable aperture sizes in sensitive high-frequency applications.

Figure 9 illustrates the coupled degradation of SE as a function of both the number of apertures and the logarithm of frequency, helping us to see the rapid decline in performance across these parameters.

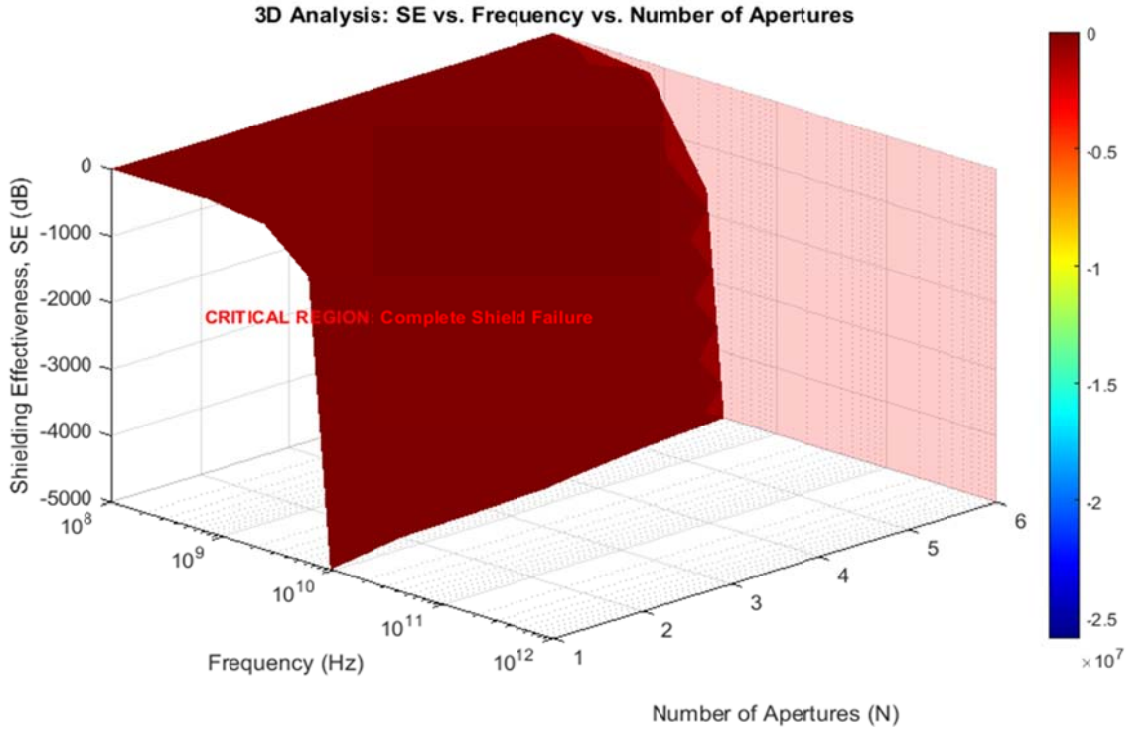

Figure 8: SE Coupled Degradation

This plot is important as it reveals that the impact of multiplying apertures is not constant but is amplified with increasing frequency, highlighting the acute vulnerability of shields with multiple openings in high-frequency regimes.

5. Conclusion

This investigation reveals that the shielding effectiveness (SE) of an enclosure is influenced not only by the intrinsic properties of its base material but is also significantly and non-linearly compromised by the presence of apertures. The study highlights that the quantity, dimensions, and geometry of these openings are critical design parameters. A consistent trend emerges: as the number of apertures (N) increases, SE declines markedly, an effect that intensifies at higher operational frequencies. Notably, elongated openings such as slots pose a greater threat to shielding integrity than circular or square apertures of equivalent area. Consequently, design strategies should prioritise circular interface configurations to mitigate electromagnetic leakage.

These results carry major considerations for future communication hardware and feed directly into the 3GPP's current discussions on 6G band channel plans for 7GHz [28]. Early proposals assumed channel widths as large as 10 GHz, but the shift toward 200 MHz allocations has laid bare the real-world engineering hurdles, of which chief among them is effective electromagnetic containment. Even with narrower bandwidths, terahertz frequencies demand enclosures that are virtually leak-proof across the entire spectrum. Our analysis demonstrates that the conventional approach of using multiple apertures for ventilation or cable routing simply won't suffice. Instead, designers must adopt an integrated mindset, of treating the shield as a single electromagnetic system and ensuring each opening is precisely controlled or eliminated. Achieving this will rely on advanced methods such as embedding electromagnetic band-gap (EBG) structures, applying frequency-selective surface (FSS) treatments, and employing waveguides below apertures to maintain RF front-end integrity. Whether operating over 200 MHz slices or full 10 GHz spans, terahertz signals' acute sensitivity to aperture leakage makes next-level shielding strategies indispensable for 6G. As research are ongoing in the areas of interference mitigation [29], [30] and [31], there is also the need to pay attention to device-to-device interference caused due to aperture utilisation.

References

[20] Afilipoaei, C., & Teodorescu-Draghicescu, H. (2020). A review over electromagnetic shielding effectiveness of composite materials. *Proceedings of the 14th International Conference on Interdisciplinarity in Engineering—INTER-ENG 2020*, Târgu Mureș, Romania, 8–9 October 2020, 1–9.

https://dx.doi.org/10.3390/proceedings2020063023

[4] ASTM International. (2018). *Standard test method for measuring the electromagnetic shielding effectiveness of planar materials (ASTM D4935-18)*. https://webstore.ansi.org/Search/Find?in=1&st=ASTM+D4935-18

[8] Basyigit, I. B., Dogan, H., & Helhel, S. (2019). The effect of aperture shape, angle of incidence and polarization on shielding effectiveness of metallic enclosures. *Journal of Microwave Power and Electromagnetic Energy*, 53(2), 115–127. https://doi.org/10.1080/08327823.2019.1607496

[11] Xueping Xu, Wei Liu, Yuejing Huang, Wangchang Li, & Shenglei Che (2023). Magnetic shielding mechanism and structure design of composites at low frequency: A review. Journal of Magnetism and Magnetic Materials 570(23):170509. DOI: 10.1016/j.jmmm.2023.170509

[18] Bethe, H. A. (1944). Theory of diffraction by small holes. *Physical Review*, 66(7–8), 163–182. https://doi.org/10.1103/PhysRev.66.163

[17] Cadence System Analysis. (n.d.). The size of apertures and the EMI shield wavelength. https://resources.system-analysis.cadence.com/blog/msa2021-the-size-of-apertures-and-the-emi-shield-wavelength

[9] Cakir, M., Kockal, N., Ozen, S., Kocakusak, A., & Helhel, S. (2017). Investigation of electromagnetic shielding and absorbing capabilities of cementitious composites with waste metallic chips. *Microwave Power and Electromagnetic Energy*, 51(1), 31–42.

[10] Dehkhoda, P., Tavakoli, A., & Azadifar, M. (2012). Shielding effectiveness of an enclosure with finite wall thickness and perforated opposing walls at oblique incidence and arbitrary polarization by GMMoM. *IEEE Transactions on Electromagnetic Compatibility*, 54(4), 792–805. https://doi.org/10.1109/TEMC.2011.2178856

[22] Dřínovský, J., & Kejík, Z. (2009). Electromagnetic shielding efficiency measurement of composite materials. *Measurement Science Review*, 9(4), 109–112. https://doi.org/10.2478/v10048-009-0020-8

[7] Erdumlu, N., & Saricam, C. (2015). Electromagnetic shielding effectiveness of woven fabrics containing cotton/metal-wrapped hybrid yarns. *Journal of Industrial Textiles*, 46(4), 1084–1103. https://doi.org/10.1177/1528083715613628

[15] Güler, S. (2023). An investigation on electromagnetic shielding effectiveness of metallic enclosure depending on aperture position. *Journal of Microwave Power and Electromagnetic Energy*, 57(2), 129–145. https://doi.org/10.1080/08327823.2023.2209477.

[25] Huang C. & Mao, J. (2019). Polarizabilities of Apertures of Various Shapes and Their Applications to Shielding Effectiveness," *in IEEE Transactions on Electromagnetic Compatibility*, 2019. (This paper provides a modern review and calculations for various shapes).

[23] IEEE. (1998). *IEEE standard method for measuring the effectiveness of electromagnetic shielding enclosures* (IEEE Std 299-1997). https://doi.org/10.1109/IEEESTD.1998.88115

[1] IEEE. (2007). *IEEE standard method for measuring the effectiveness of electromagnetic shielding enclosures* (IEEE Std 299-2006). https://doi.org/10.1109/IEEESTD.2007.364646

[14] Kihal, M. C., Chebout, M., Sekki, D., Kihal, M., Azizi, H., & Moulai, H. (2024). Electromagnetic coupling evaluation of small metal enclosures with apertures using analytical, numerical and measurement analysis. *South Florida Journal of Development*, 5(11), 1–12.

[5] Kwon, J. H., Hwang, J. H., & Park, H. H. (2019). Improving shielding effectiveness of enclosure with apertures using absorbers. *2019 IEEE International Symposium on Electromagnetic Compatibility, Signal & Power Integrity (EMC+SIPI)*, 356–359. https://doi.org/10.1109/ISEMC.2019.8825201

[2] Kwon, J. H., Hyoung, C. H., Hwang, J.-H., & Park, H. H. (2021). Impact of absorbers on the shielding effectiveness of metallic rooms with apertures. *Electronics*, 10(3), 237. https://doi.org/10.3390/electronics10030237

[16] Leadertechnic. (n.d.). How apertures affect EMI shielding. https://leadertechinc.com/how-apertures-affect-emi-shielding.

[21] Marvin, A. C., Dawson, L., Flintoft, I., & Dawson, J. (2009). A method for the measurement of shielding effectiveness of planar samples requiring no sample edge

preparation or contact. *IEEE Transactions on Electromagnetic Compatibility*, 255–262. https://doi.org/10.1109/TEMC.2009.2015147

[26] McDonald, N. A. (1972). Electric and magnetic coupling through small apertures in shield walls. IEEE Transactions on Electromagnetic Compatibility, EMC-14(1), 2-6. https://doi.org/10.1109/TEMC.1972.303156

[3] MIL-DTL-83528F. (2018). *Gasketing material, conductive, shielding gasket, electronic, elastomer EMI/RFI general specifications for*. http://everyspec.com/MIL-SPECS/MIL-SPECS-MIL-DTL/MIL-DTL-83528F_52728/

[13] Orasugh, J. T., & Ray, S. S. (2023). Functional and structural facts of effective electromagnetic interference shielding materials: A review. *ACS Omega*, 8(9), 8134–8158. https://doi.org/10.1021/acsomega.2c05815

[24] Robinson, M. P., Benson, T. M., Christopoulos, C., Dawson, J. F., Ganley, M. D., & Marvin, A. C. (1998). Analytical formulation for the shielding effectiveness of enclosures with apertures. *IEEE Transactions on Electromagnetic Compatibility*, 40(3), 240–248. doi:10.1109/15.709422

[19] Robinson, M. P., Turner, J. D., Thomas, D. W. P., Dawson, J. F., Ganley, M. D., Marvin, A. C., Porter, S. J., & Benson, T. M. (1996). Shielding effectiveness of a rectangular enclosure with a rectangular aperture. *Electronics Letters*, 32(17), 1559–1560.

[12] Sezer, N., Arı, İ., Biçer, Y., & Koç, M. (2021). Superparamagnetic nanoarchitectures: Multimodal functionalities and applications. *Journal of Magnetism and Magnetic Materials*, 538, 168300. https://doi.org/10.1016/j.jmmm.2021.168300

[28] THALES. What are the latest developments on 6G?, https://www.thalesgroup.com/en/worldwide-digital-identity-and-security/mobile/magazine/what-are-latest-developments-6g#:~:text=In%20December%202024%2C%203GPP%20decided,higher%20frequencies%20for%20defence%20purposes.

[27] Xu, X., Liu, W., Huang, Y., Li, W., & Che, S. (2023). Magnetic shielding mechanism and structure design of composites at low frequency: A review. *Journal of Magnetism and Magnetic Materials*, 570, 170509. https://doi.org/10.1016/j.jmmm.2023.170509

[6] Yin, J., Ma, W., Gao, Z., Lei, X., & Jia, C. (2022). A review of electromagnetic shielding fabric, wave-absorbing fabric and wave-transparent fabric. *Polymers*, 14, 377. https://doi.org/10.3390/polym14030377.

[29] R.A. Udoh, U.S. Ukommi, and E.A. Ubom, "Evaluation of modified artificial neural network-based interference mitigation in 5G network," Sci. Technol. Publ. (SCI & TECH), vol. 7, no. 12, pp. 1604–1613, 2023.

[30] R.A. Udoh, U.S. Ukommi, and E.A. Ubom, "Interference mitigation in 5G network using frequency planning and artificial neural network (ANN)," J. Multidiscip. Eng. Sci. Technol. (JMEST), vol. 10, no. 12, pp. 16534–16540, 2023.

[31] C.O. Uloh, E.A. Ubom, A.U. Obot, and U.S. Ukommi, "Interference mitigation and power consumption reduction for cell edge users in future generation networks," J. Eng. Res. Rep., vol. 26, no. 2, pp. 89–106, 2024.